

Experimental Investigation of Static Properties of Magnetorheological Elastomer

**Nor F. Alias, Asan G.A. Muthalif,
Khairul A.M. Arpan & N. H. Diyana
Nordin**

**Iranian Journal of Science and
Technology, Transactions of
Mechanical Engineering**

ISSN 2228-6187

Iran J Sci Technol Trans Mech Eng
DOI 10.1007/s40997-017-0081-5



Your article is protected by copyright and all rights are held exclusively by Shiraz University. This e-offprint is for personal use only and shall not be self-archived in electronic repositories. If you wish to self-archive your article, please use the accepted manuscript version for posting on your own website. You may further deposit the accepted manuscript version in any repository, provided it is only made publicly available 12 months after official publication or later and provided acknowledgement is given to the original source of publication and a link is inserted to the published article on Springer's website. The link must be accompanied by the following text: "The final publication is available at link.springer.com".

Experimental Investigation of Static Properties of Magnetorheological Elastomer

Nor F. Alias¹ · Asan G.A. Muthalif¹ · Khairul A.M. Arpan¹ · N. H. Diyana Nordin¹

Received: 27 June 2016 / Accepted: 27 April 2017
© Shiraz University 2017

Abstract Magnetorheological elastomer (MRE) is a type of smart material made of natural or synthetic rubber filled with micron-sized magnetic particles. Its shear modulus and elasticity can be controlled by applying an external magnetic field. In this study, a mounting system model is used to obtain displacement transmissibility factor. In the experimental analysis, three different MRE samples are manufactured by varying the percentage of magnetic particles. The experimental investigations are carried out to characterize the quasi-static properties of these MREs by attaching them with universal testing machine in compression and tensile mode. In both modes, different currents and velocities are applied to the samples. From the experimental results, a proportional relationship has been observed among the resisting force from MREs and applied excitation current, displacement and velocity. In most cases, the force has increased with the increasing percentage of magnetic particles in the sample. However, the highest force is obtained from the sample with 30% magnetic particles, at 2 A current and velocity of 4 mm/min. The results observed in this research would be useful for vibration control in applications such as engine mounting system.

Keywords Quasi-static properties · Mounting system model · Magnetorheological elastomer · Transmissibility factor

1 Introduction

Magnetorheological materials are a kind of smart materials which could be in the form of fluid, gel or even a solid material like elastomers. Magnetorheological elastomer (MRE), which is a member of MR material family, is an intelligent material having physical properties that can be reversible and instantaneously controlled by an external magnetic field. Usually, MREs are composite materials, where micron-sized (typically 3–5 microns) ferromagnetic particles are suspended within a non-magnetic natural or synthetic rubber matrix (Carlson and Jolly 2000; Jolly et al. 1996). When magnetic field is applied to the MRE, the suspended ferromagnetic particles show an MR effect and become semi-solid from soft foam with regard to the strength of applied field (Chen et al. 2007; Li et al. 2014; Sutrisno et al. 2015). The rheological properties of these materials are rapidly and reversibly altered in the absence of magnetic field. These features mark the MRE as an adaptive stiffness element (Hashi et al. 2016). In addition, MRE exhibits magnetodielectric effects as discussed in Bica et al. (2015).

The MREs are capable of overcoming the limitations of another MR family member named MR fluids like sedimentation of magnetic particles dispersed in the fluid environmental contagion. Combining the advantages of magnetorheological fluids and elastomers, MREs have attracted many researchers, making it an ideal possibility for different vibration control applications like engine mounting system (Cao and Deng 2009), automobile

✉ Asan G.A. Muthalif
asan@iium.edu.my

N. H. Diyana Nordin
norhidayati.nordin@gmail.com

¹ Smart Structures, Systems and Control Research Laboratory (S3CRL), Department of Mechatronics Engineering, International Islamic University Malaysia, Jalan Gombak, 53100 Kuala Lumpur, Malaysia

suspensions (Yu et al. 2001), seat suspensions (Du et al. 2011), clutches (Li et al. 2012), robotics, design of buildings and bridges (Li and Li 2015), home appliances like washing machines (Yang et al., 2013). In the automotive industry, passive engine mounting is generally used to support the engine on the chassis and at the same time to isolate vibration from the engine. These passive engine mounts are unable to isolate the shock and vibration completely, where the active mount performs much better than the passive one. However, their configuration is complex and requires huge amounts of power. To solve all these problems, new MRE-based semi-active engine mounts are proposed by many researchers (Popp et al. 2010) as they can perform as well as active mounts with simple configuration, lower implementation cost, are easier to control and install, and consume comparatively less power.

Numerous techniques are anticipated to investigate the performance of MREs. For instance, Ginder et al. (Arzandpour and Golnaraghi 2008; Ginder et al. 2002) of the Ford Research Laboratory analyzed average magnetic induction using finite element analysis and calculated the shear stresses from the field using Maxwell's stress tensor. By considering the magnetic interactions between two adjacent particles, Jolly et al. (1996) proposed a modified version of a simple dipole model for estimating the MREs performance. Davis (1999) has considered the interactions in a single particle chain in order to calculate the saturated field induced shear modulus. Gong et al. (2005) have carried out a research with multiple MRE samples with varying percentage of carbonyl iron particles. Another approach of increasing MR effect is using comparatively bigger iron particles. Bose and Roder (Böse and Röder 2009) exposed the effects of larger iron particles in the cross-linking of silicone and found a lower value of elasticity in that composite. From their research, they discovered that the MREs with large iron particles having a size of 40 μm can produce a 20 times higher MR effect as compared to the normal sized iron particles which are able to induce MR effect fluctuating from 0.05 to 5 times

(Liao et al. 2012; Opie and Yim 2010; Tian et al. 2011). The majority of the models are accurate enough to predict the MR effects produced by implanted ferromagnetic elements. However, the properties of an MRE cannot be comprehensively characterized by only considering the MR effect induced by the ferromagnetic particles. The matrix of MRE has an influence on the MR effect. The effects of the polymer matrix and its interaction with embedded particles also play an important role in establishing MRE performance. Shen et al. (2004) have used two different materials such as natural rubber and polyurethane as matrices of MRE in their research. Their experimental results clearly show the ability of different matrices to alter the MR effect, where the MRE sample with natural rubber induced 20% MR effect and another sample with polyurethane sealant produced a higher MR effect (150%). Wang et al. (2006) investigated on different matrices of MRE in their research and found that MRE sample having lower initial storage modulus (G_0) induces larger MR effect. They have advised a soft matrix be used to make MRE with greater MR effect. Thus, it is possible to maximize MR effect of MRE through design optimization.

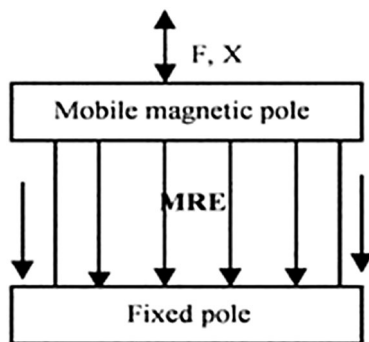


Fig. 1 Squeeze mode of operation in MRE

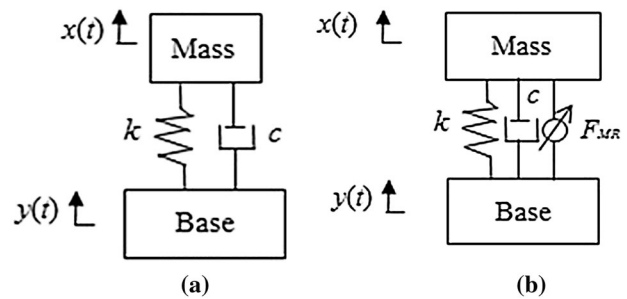


Fig. 2 Mathematical model of a passive system and b semi-active system

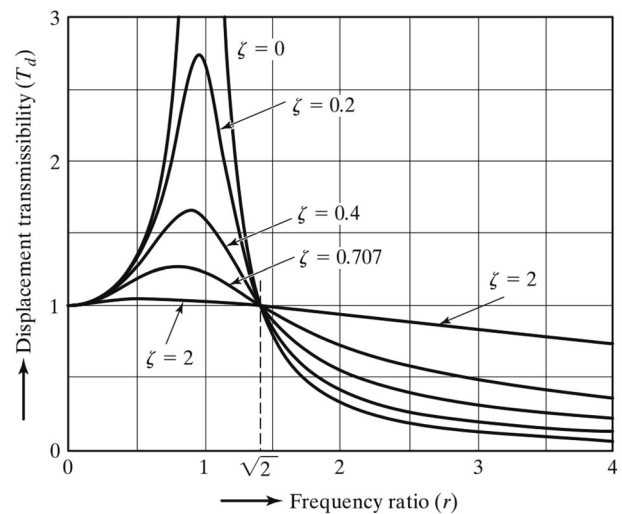


Fig. 3 Transmissibility diagram (Rao 2011)

An MRE component is commonly subjected to dynamic loading in various engineering applications, where the amplitude and frequency of this dynamic loading greatly affect MREs mechanical properties, such as shear modulus and damping ratio. In this research, three different MRE samples have been developed by mixing 20, 30 and 40% of ferromagnetic particles with natural rubber. Dynamic properties of those samples are investigated with universal testing machine (UTM) and studied under various modes. Mainly, the resisting force from MREs at different velocity and excitation current is explored to characterize their dynamic properties.

This paper consists of four sections. Section 1 gives a brief background on the researches related to MREs, where analytical modeling of the MRE in semi-active system is presented in Sect. 2. Section 3 discusses the work done in this paper, which involves experimental studies and data analysis. The conclusion is presented in Sect. 4.

2 Analytical Modeling

In analyzing the static behavior of the system, mathematical modeling of the whole system is first derived. The model can then be used to evaluate the controller performance before implementing on the real system. By changing the physical properties of the MR elastomer, its stiffness capability can be varied. The physical properties are changed by the application of magnetic field, where the rubber becomes stiffer at higher magnetic flux density. A series of copper wires are coiled around the rubber. These coils are capable of generating magnetic flux and thus induce magnetic field inside the MRE. The magnetic field intensity is controlled by tuning the amount of current to be supplied from a DC supply, which acts as the supervisor of the entire system. Universal testing machine (UTM) is used to characterize the MRE by supplying compression and tensile force. This MRE-based model works as a semi-active control system, where the MRE behaves like a passive spring in off mode and becomes rigid in an active mode in the presence of magnetic field. A change in the stiffness is obtained with the increasing magnetic field intensity. The direction of the applied force from the UTM is parallel to the induced magnetic field direction and goes through the MRE in accordance with the force direction. MRE in squeeze mode is shown in Fig. 1.

In the engine mounting system, the uneven road surface applies excitation force on the vehicle body and causes vibration which directly affects the engine. In this work, the road excitation is assumed to be in a simple harmonic motion form and only vertical vibration is taken into consideration. The mounting system can be modeled as a

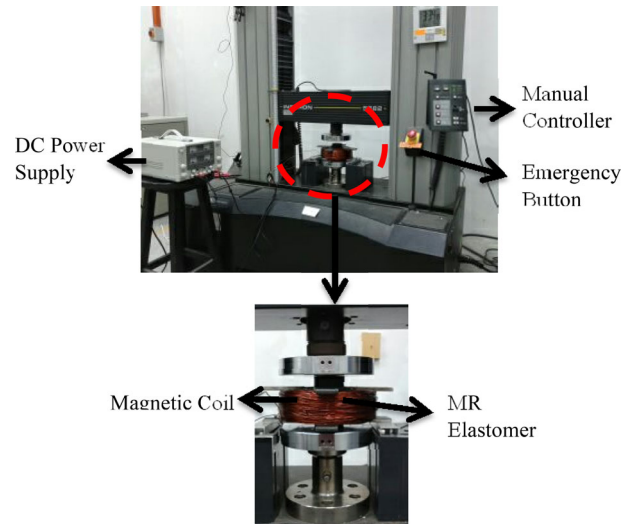


Fig. 4 Experimental setup

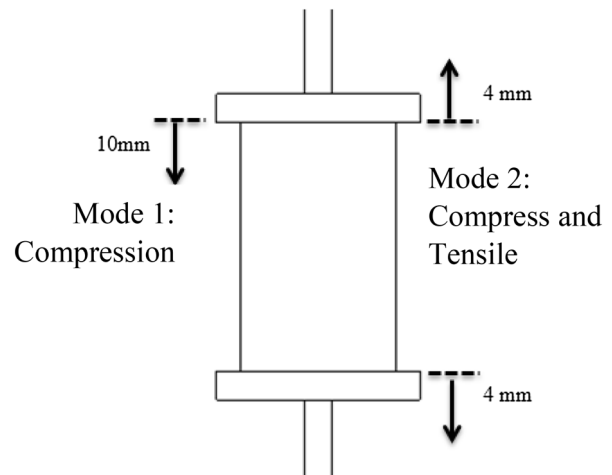


Fig. 5 Testing setup at mode 1 and mode 2

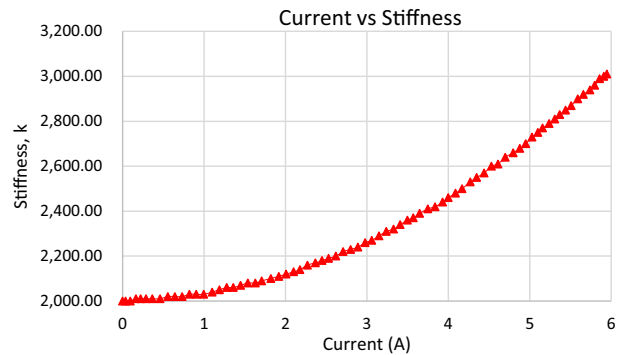


Fig. 6 Stiffness of MRE versus applied current

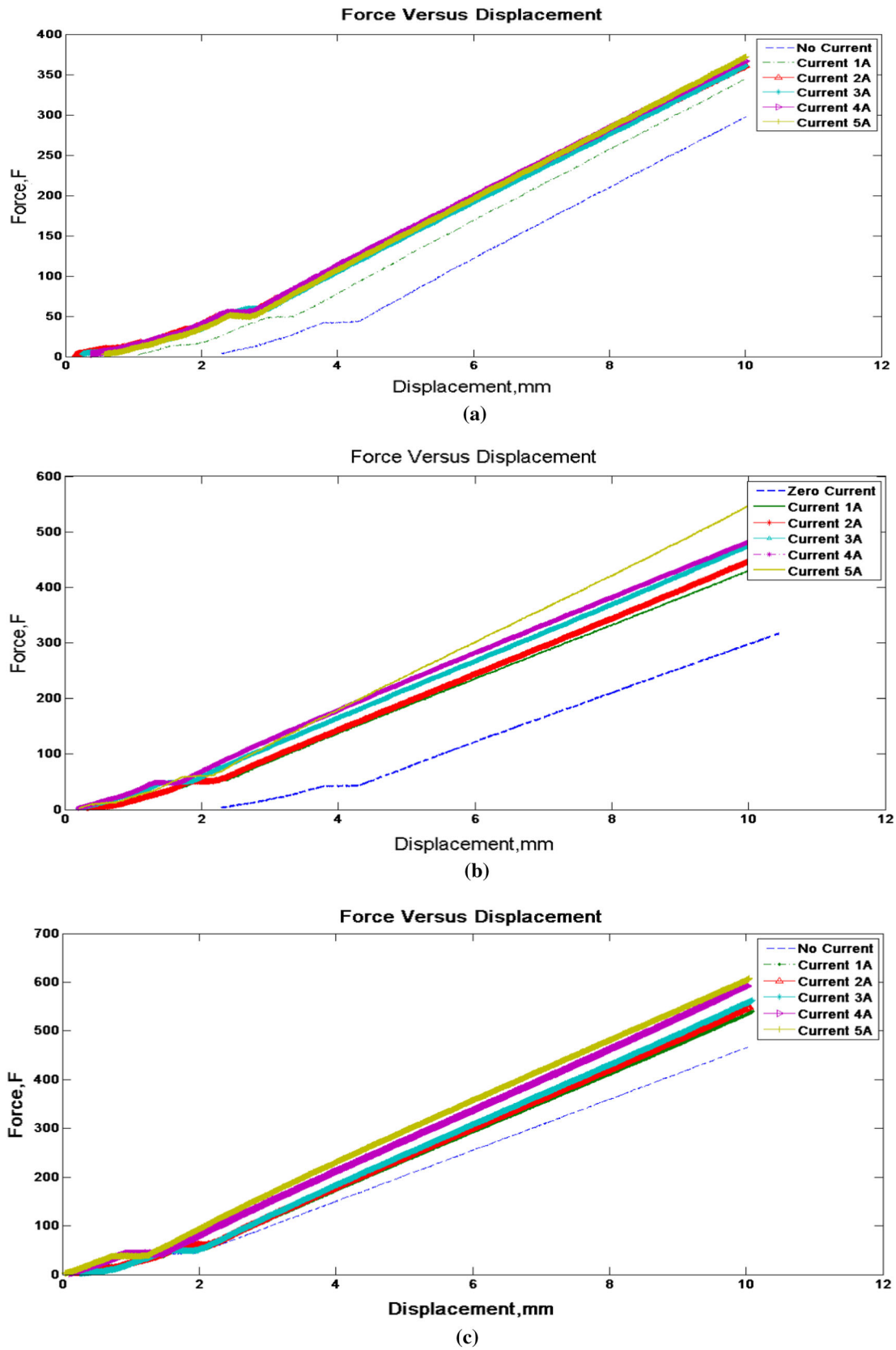


Fig. 7 Experimental results of compression mode (10 mm) with velocity 2 mm/min for different percentage of magnetic particles: **a** Sample 1, **b** Sample 2 and **c** Sample 3

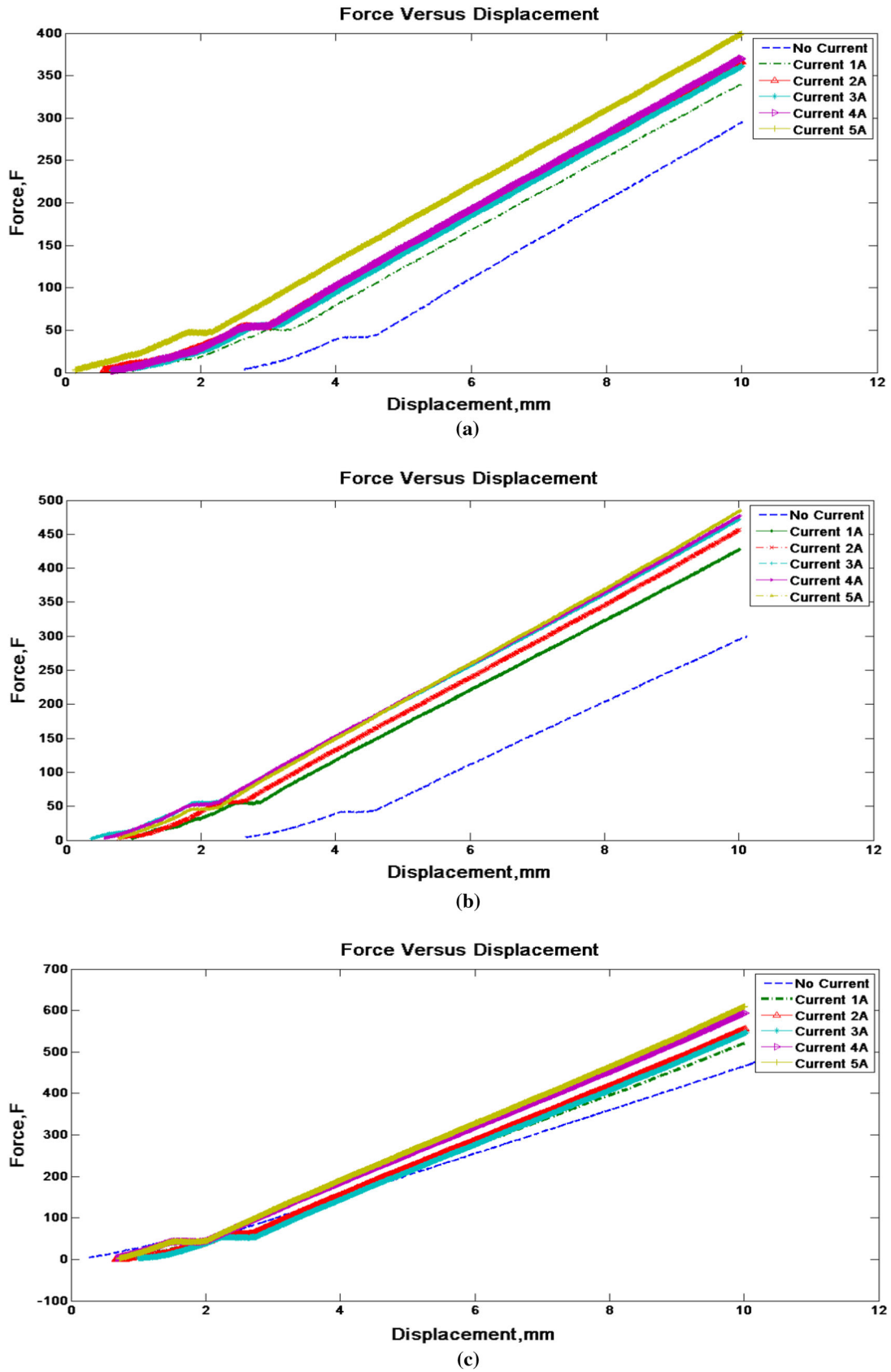


Fig. 8 Experimental results of compression mode (10 mm) with velocity 4 mm/min for a Sample 1, b Sample 2 and c Sample 3

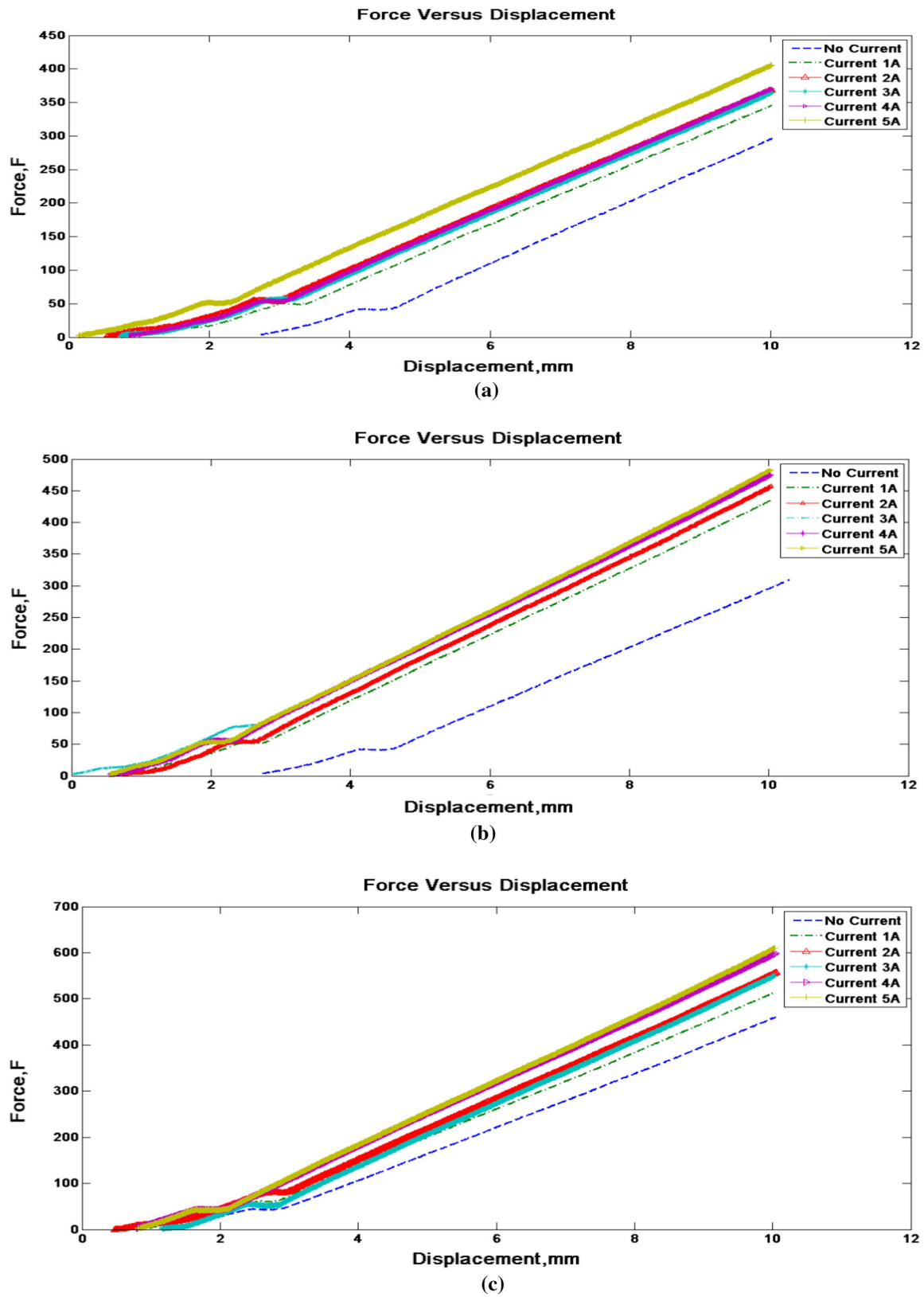


Fig. 9 Experimental results of compression mode (10 mm) with velocity 6 mm/min for a Sample 1, b Sample 2 and c Sample 3

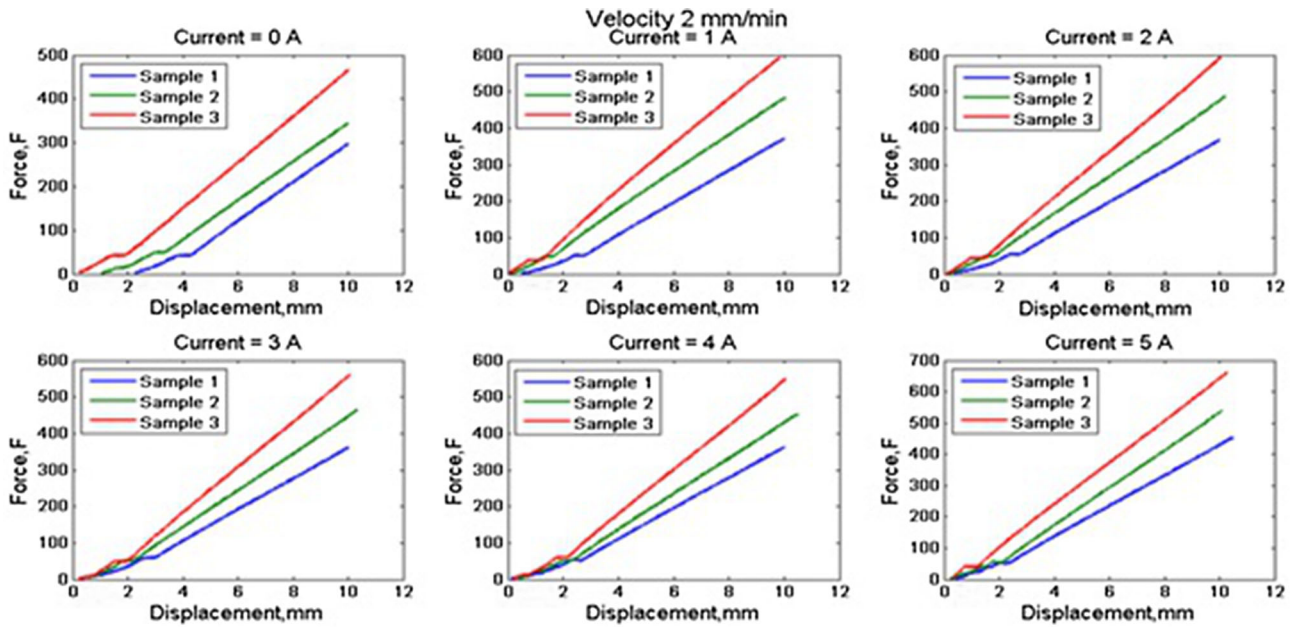


Fig. 10 Comparison stiffness for different samples at different current for a velocity of 2 mm/min

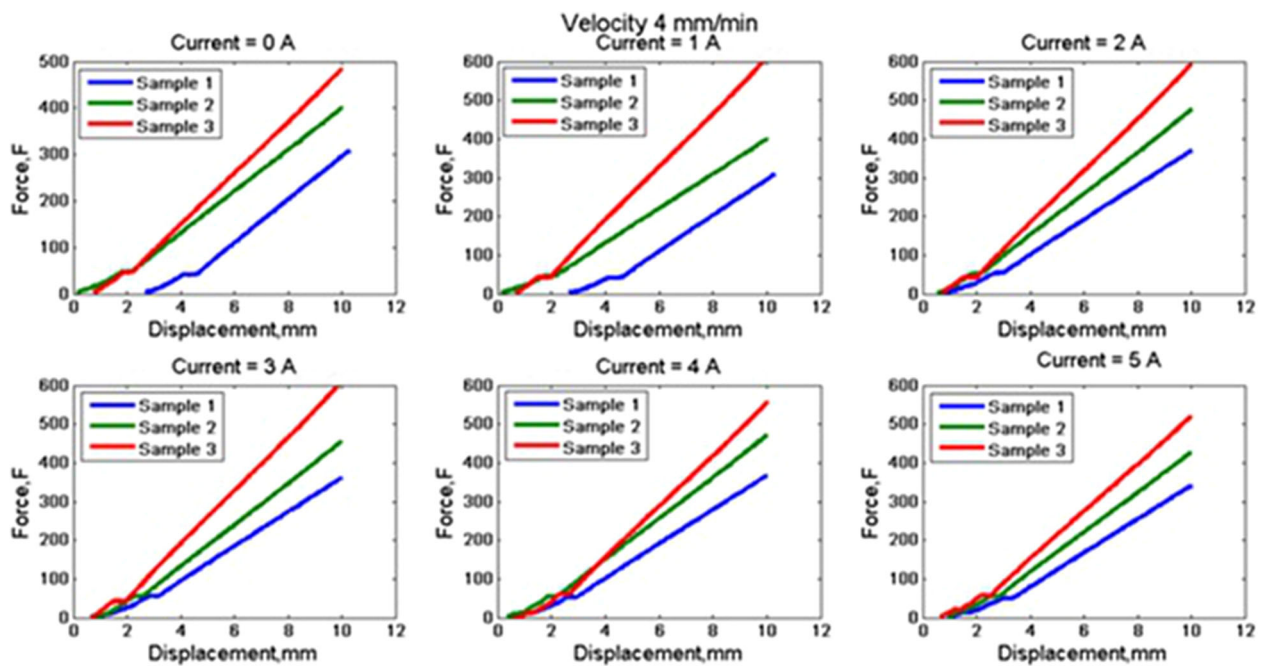


Fig. 11 Comparison stiffness for different samples at different current for a velocity of 4 mm/min

simple base excited one degree of freedom system as shown in Fig. 2.

The equation of motion of the system can be defined as

$$m\ddot{x} + c\dot{x} + kx + F_{MR} = c\dot{y} + ky \quad (1)$$

In this form, the dynamics of the system is modeled in terms of stiffness, k , damping, c , the base input displacement, y , and relative output upper mass

displacement, x . Applying Newton's law of motion to both the engine mass and the base and substituting it into Eq. (1) lead to

$$m\ddot{x} + c\dot{x} + k'x = c\dot{y} + k'y \quad (2)$$

where

$$k' = k + k_{MR} \quad (3)$$

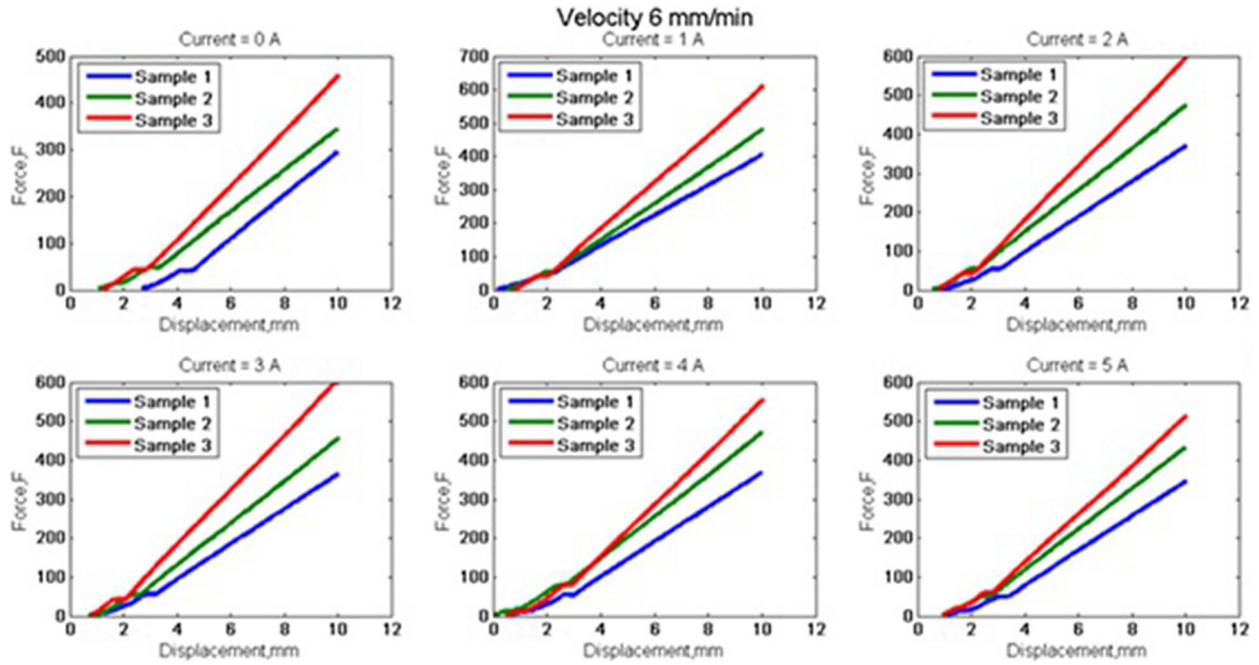


Fig. 12 Comparison stiffness for different samples at different current for a velocity of 6 mm/min

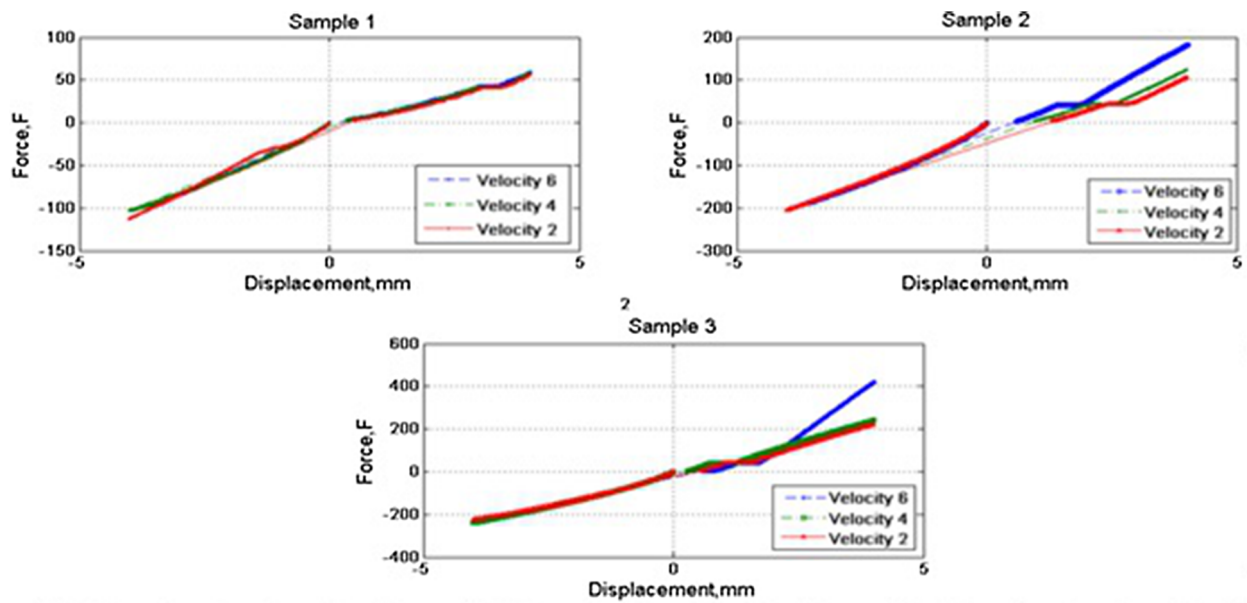


Fig. 13 Force versus displacement plot of Sample 1, Sample 2 and Sample 3

Here, c and k' are the rubber damping and stiffness coefficients, respectively.

Using $s = j\omega$, the transfer function of the system can be defined as in Eq. (4) as:

$$\frac{X(j\omega)}{Y(j\omega)} = \frac{cj\omega + k'}{m(j\omega)^2 + cj\omega + k'} \quad (4)$$

The displacement transmissibility, T , which is the ratio of the amplitude of the response $x(t)$ to that of the base motion $y(t)$, is written as

$$T = \left| \frac{X(\omega)}{Y(\omega)} \right| = \sqrt{\frac{(c\omega)^2 + (k + k_{MR})^2}{(c\omega)^2 + (k + k_{MR} - m\omega^2)^2}} \quad (5)$$

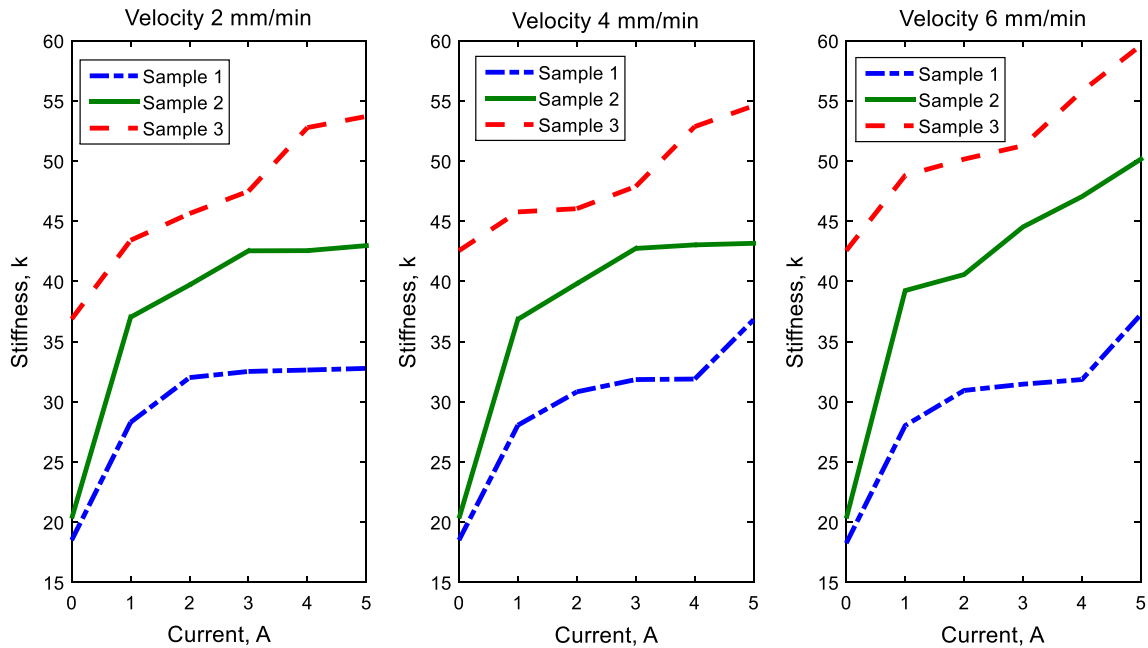


Fig. 14 Relationship between stiffness and current for three different samples at different velocity

In developing an MRE assist isolator, the consideration of transmissibility is an important factor. Transmissibility is the ratio of the amplitude of the response $y(t)$ to that of the base motion $x(t)$ at the same frequency f_e . Referring to Fig. 3, the frequency ratio, f/f_n , must be greater than $\sqrt{2}$ (isolation zone) and ideally greater than 2–3 in order to achieve a significant level of vibration isolation. Systems where the frequency ratio is below $\sqrt{2}$ (amplification zone) are not suitable for isolation.

3 Experimental Setup with Result Analysis

The experimental setup is comprised of MR elastomers, electromagnetic coils, DC supply and a universal testing machine (UTM) as displayed in Fig. 4.

The UTM is used to analyze the MR elastomers by providing the compression and tensile forces. The displacement of the rubber is measured by a linear variable differential transformer (LVDT) sensor, integrated with the UTM. During the experiment, a variable current was supplied to magnetic coils to induce magnetic field in the rubber. The required signal was generated using Instron BlueHill software running on a computer, and the data were obtained from the software. The force and the displacement were analyzed for different velocities and different starting positions of the rubber. The testing mode is divided into two parts, where mode 1 starts from zero and compresses until 10 mm. Mode 2 starts from zero point and has 4 mm cyclic movement (compression and tension) as shown in Fig. 5.

From Fig. 6, it is clearly observed that when the current increases, the stiffness increases accordingly. In the presence of a magnetic field, the particles inside the elastomer are aligned to form head-to-tail chains. The increasing applied current intensifies the magnitude of magnetic field and strengthens those chains in the MRE. Consequently, it increases the stiffness, making the elastomer stiffer.

In this research, several experiments were carried out to analyze the MREs behavior. Three MRE samples containing different amounts of magnetic particles are used for this purpose. Sample 1 contains 20% magnetic particles, Sample 2 with 30% magnetic particles and Sample 3 consists of 40% magnetic particles. At the beginning of the experiment, the UTM is set to operate in both compression and tensile mode. The data from INSTRON BLUEHILL are obtained and plotted to observe the different types of relationship such as forces exerted by the MREs which are observed for various current supplied to MREs at 4 mm distance in both tensile and compression mode, and at 10 mm distance at compression mode. Further, the force delivered by all three MRE samples for variable velocity of 2, 4 and 6 mm/min is examined.

3.1 Result Analysis for Mode 1 (10 mm Compression)

In this mode 1, UTM applies 10 mm compression to the MREs. Forces are observed for 0–5 A applied current with an increment of 1 A. The velocities are changed from 2 mm/min, followed by 4 mm/min and finally, 6 mm/min, results of which are shown in Figs. 7, 8 and 9, respectively.

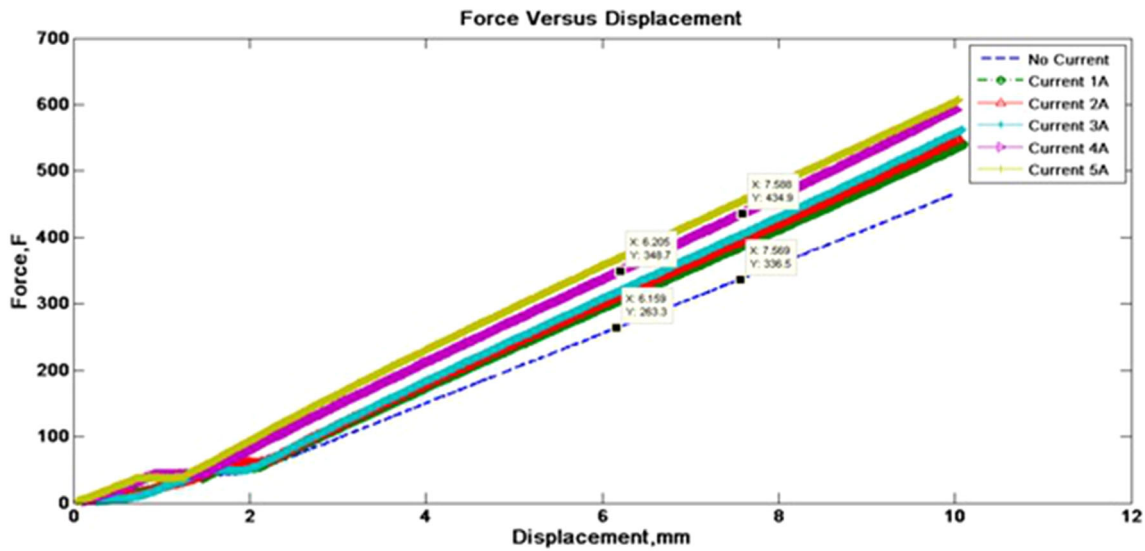
In Fig. 7a–c, forces are plotted for velocity of 2 mm/min with variable excitation current from 0 to 5 A for the three MRE samples.

In Fig. 7, for all three samples, the forces have proportional relation with the excitation current. As the percentage of magnetic particles has increased, the maximum force value has increased and the highest force is obtained from Sample 3 (40% magnetic particles), which is very close to 600 N.

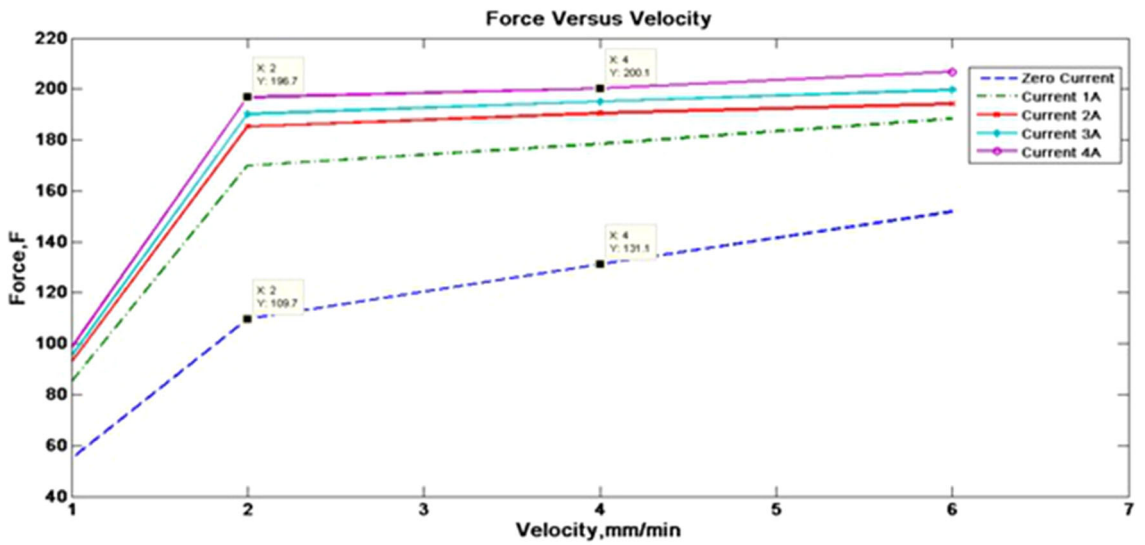
In Fig. 8, the velocity is 4 mm/min, and the velocity is 6 mm/min in Fig. 9. In both figures, the forces are examined and plotted for 10 mm compression mode for all three

different MRE samples. The supply currents are also varied from 0 to 5 A.

In mode 1 (10 mm compression mode), most of the graphs show that the forces are not so stable at the beginning. However, after a certain distance the forces increase rapidly to the extension point of 10 mm. The forces are seen to increase linearly with the current. The particles are aligned linearly in a rigid chain structure for higher current due to the corresponding increment in magnetic field. Thus, more mechanical energy is needed to press the chain-like structures rigid structure. During compression mode, the rubber tends to reposition due to its



(a)



(b)

Fig. 15 Stiffness and damping factor expression for minimum and maximum value. a Force versus displacement. b Force versus velocity

elasticity. This tendency is intensified as displacement increases and consequently more forces are induced, which is witnessed in Figs. 8, 9 and 10. Another interesting point of observation is that every sample consists of a different percentage of magnetic particles delivering different forces when current is induced to the coil. The responses in Figs. 7, 8 and 9 are observed, and different maximum force is obtained at each sample. The maximum force for the first sample is the smallest, while the maximum force for Sample 3 is greater than Sample 2 in all velocities of 2, 4 and 6 mm/min.

For a certain velocity, the comparison of delivered forces among three MRE samples at different currents is presented in Figs. 10, 11 and Fig. 12 for mode 1. Figure 10 is for velocity 2 mm/min, Fig. 11 is run at velocity 4 mm/min, and Fig. 12 is for velocity 6 mm/min.

In all cases, the Sample 3 exhibits the highest force. This is because the existence of more magnetic particles inside the rubber results in more resistance by forming a thicker chain column in the direction of magnetic field. Thus, the rubber becomes stiffer and requires more force to break the resistance to compress the rubber.

3.2 Result Analysis for Mode 2 (4 mm Cyclic Mode)

Mode 2 is a cyclic mode which combines 4 mm tensile and compression mode. In this mode, all three MRE samples' forces are analyzed for different velocities of 2, 4 and 6 mm/min, as presented in Fig. 13.

From the results presented in Fig. 13, it is obvious that experimental force delivered by the MRE samples is always proportional to the velocity applied to rubber, i.e.,

the forces are slightly higher when velocity is increasing. Since this experimental mode is tested for different magnetic composition for every sample, the force needed is also different, which is higher as the magnetic percentage increases under tensile and compression mode. The area of the hysteresis loop is the energy consumed through the cycle mode. For MR elastomer, the hysteresis loop in the presence of magnetic field is different from the loop in absence of magnetic field. This is due to the magnetic viscoelasticity. The same thing happens for different magnetic particles composition in the MR elastomer.

The stiffness has been experimentally measured and plotted for excitation current varying from 0 to 5 A for all the MRE samples and for varying velocity from 2 to 6 mm/min with an increment of 2 mm/min, which are displayed in Fig. 14.

Figure 15 shows that the elasticity force increases with the rising value of input current. The dynamic behavior of MR elastomer is investigated by changing parameters in rheological model to influence the performance of the composite.

The slope for the force–displacement and force–velocity curves is observed in Fig. 15.

In Fig. 15, it is seen that the slope of graph at zero current has the minimum value, whereas the slope of graph at current 4A shows the maximum value. Thus, by controlling the stiffness and damping factor according to the excitation frequency, the optimized vibration control effect will be obtained.

After further analysis, Fig. 16 represents the relationship between force and velocity to determine the optimal force for specific amount of magnetic particles in the sample. For

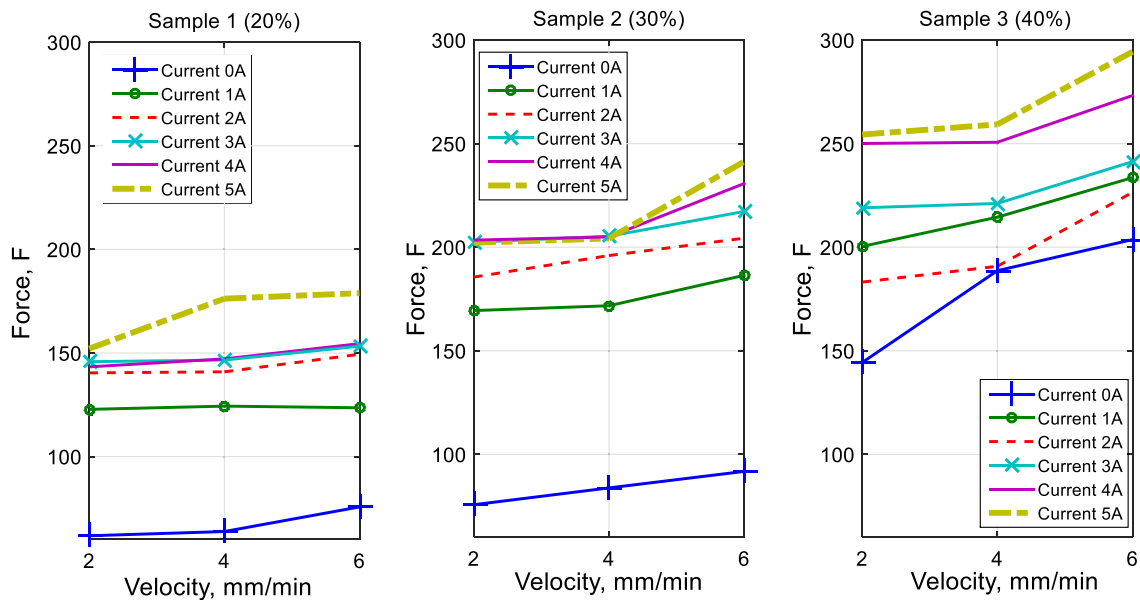


Fig. 16 Relationship between force and velocity for different samples at different velocities

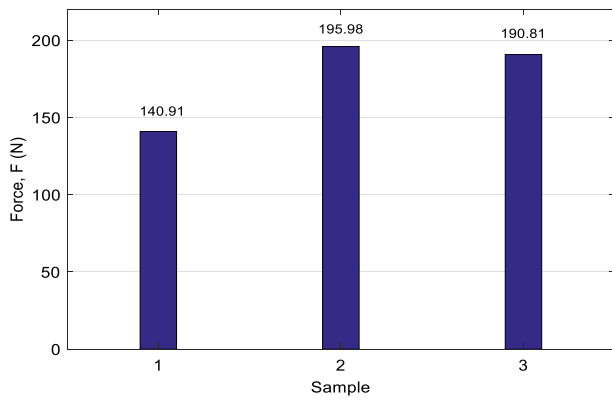


Fig. 17 Optimal force at velocity 4 mm/min, observed at 2 A of current

most cases, the force has increased with increasing amount of percentage of magnetic particles in the sample. However, in Fig. 17 the graph shows that highest value of force is obtained at current 2 A with velocity 4 mm/min, which proves that the optimal sample is Sample 2 with 30% of magnetic particles at this specific velocity of 4 mm/min with applied current of 2 A. From the above investigation, the results would be useful for vibration control and set as a benchmark to implement in real application.

4 Conclusion

Magnetorheological elastomer is a smart material with stable and controllable mechanical properties. The idea of using MRE for vibration control application such as in engine mounting system is known to be effective. This research experimentally investigated the static and quasi-static behavior of MR elastomer for semi-active vibration control, where tests have been performed to determine the properties of MRE. The sensitivity parameters are evaluated such as mount stiffness, loading speed and applied magnetic field in order to determine the influence of parameters on vibration isolation. The results are investigated from the relationship between the force and compression displacement as well as the relationship between the force and velocity. The properties are controlled by changing the magnetic field with application of various current. Thus, current is identified as an important parameter. The goal of this research is to obtain the desired and achieved stiffness of MRE by experimental investigation. Through proper control of the applied current into the system, the response to identify optimal mount stiffness can be enhanced. The experimental results indicate that the MRE mounting system is promising as a vibration reduction system and can be implemented in various vibration isolation applications.

Acknowledgement This work was partly supported by Exploratory Research Grant Scheme (ERGS13-020-0053) from the Ministry of Higher Education Malaysia.

References

- Arzanpour S, Golnaraghi F (2008) A novel semi-active magnetorheological bushing design for variable displacement engines. *J Intel Mater Syst Struct* 19(9):989–1003
- Bica I, Anitas E, Chirigiu L, Bunoiu M, Juganaru I, Tatu R (2015) Magnetodielectric effects in hybrid magnetorheological suspensions. *J Ind Eng Chem* 22:53–62
- Böse H, Röder R (2009) Magnetorheological elastomers with high variability of their mechanical properties. Paper presented at the *Journal of physics: Conference series*
- Cao K, Deng Y (2009) Design and analysis of an automotive vibration reduction system based on magneto-rheological elastomer. Paper presented at the *International Conference on Mechatronics and Automation. ICMA 2009*
- Carlson JD, Jolly MR (2000) MR fluid, foam and elastomer devices. *Mechatronics* 10(4):555–569
- Chen L, Gong X, Li W (2007) Microstructures and viscoelastic properties of anisotropic magnetorheological elastomers. *Smart Mater Struct* 16(6):2645
- Davis L (1999) Model of magnetorheological elastomers. *J Appl Phys* 85(6):3348–3351
- Du H, Li W, Zhang N (2011) Semi-active variable stiffness vibration control of vehicle seat suspension using an MR elastomer isolator. *Smart Mater Struct* 20(10):105003
- Ginder J, Clark S, Schlotter W, Nichols M (2002) Magnetostrictive phenomena in magnetorheological elastomers. *Int J Mod Phys B* 16:2412–2418
- Gong X, Zhang X, Zhang P (2005) Fabrication and characterization of isotropic magnetorheological elastomers. *Polym Testing* 24(5):669–676
- Hashi HA, Muthalif AG, Nordin ND (2016) Dynamic tuning of torsional transmissibility using magnetorheological elastomer: modelling and experimental verification. *Iran J Sci Technol Trans Mech Eng* 40(3):181–187
- Jolly MR, Carlson JD, Munoz BC (1996) A model of the behaviour of magnetorheological materials. *Smart Mater Struct* 5(5):607
- Li Y, Li J (2015) A highly adjustable base isolator utilizing magnetorheological elastomer: experimental testing and modeling. *J Vib Acoust* 137(1):011009
- Li W, Zhang X, Du H (2012) Development and simulation evaluation of a magnetorheological elastomer isolator for seat vibration control. *J Intel Mater Syst Struct* 23(9):1041–1048
- Li Y, Li J, Li W, Du H (2014) A state-of-the-art review on magnetorheological elastomer devices. *Smart Mater Struct* 23(12):123001
- Liao G, Gong X, Xuan S, Kang C, Zong L (2012) Development of a real-time tunable stiffness and damping vibration isolator based on magnetorheological elastomer. *J Intel Mater Syst Struct* 23(1):25–33
- Opie S, Yim W (2010) Design and control of a real-time variable modulus vibration isolator. *J Intel Mater Syst Struct* 22(2):113–125
- Popp KM, Kröger M, Li WH, Zhang XZ, Kosasih PB (2010) MRE properties under shear and squeeze modes and applications. *J Intel Mater Syst Struct* 21(15):1471–1477
- Rao SS (2011) *Mechanical vibrations*, 5th edn. Prentice Hall, Upper Saddle River

- Shen Y, Golnaraghi MF, Heppler G (2004) Experimental research and modeling of magnetorheological elastomers. *J Intell Mater Syst Struct* 15(1):27–35
- Sutrisno J, Purwanto A, Mazlan SA (2015) Recent progress on magnetorheological solids: materials, fabrication, testing, and applications. *Adv Eng Mater* 17(5):563–597
- Tian T, Li W, Alici G, Du H, Deng Y (2011) Microstructure and magnetorheology of graphite-based MR elastomers. *Rheol Acta* 50(9–10):825–836
- Wang Y, Hu Y, Chen L, Gong X, Jiang W, Zhang P, Chen Z (2006) Effects of rubber/magnetic particle interactions on the performance of magnetorheological elastomers. *Polym Testing* 25(2):262–267
- Yang J, Du H, Li W, Li Y, Li J, Sun S, Deng H (2013) Experimental study and modeling of a novel magnetorheological elastomer isolator. *Smart Mater Struct* 22(11):117001
- Yu Y, Naganathan NG, Dukkipati RV (2001) A literature review of automotive vehicle engine mounting systems. *Mech Mach Theory* 36(1):123–142